Chemical Physics Letters 681 (2017) 124–129

Contents lists available at ScienceDirect

Chemical Physics Letters

journal homepage: www.elsevier.com/locate/cplett

Research paper

Raman study of the photopolymer formation in the {Pt(dbdtc)$_2$}·C_{60} fullerene complex and the decomposition kinetics of the photo-oligomers

K.P. Meletov [a], G. Velkos [b], J. Arvanitidis [b,*], D. Christofilos [c], G.A. Kourouklis [c]

[a] Institute of Solid State Physics of RAS, Chernogolovka, Moscow region 142432, Russia
[b] Physics Department, Aristotle University of Thessaloniki, 54124 Thessaloniki, Greece
[c] Chemical Engineering Department, Aristotle University of Thessaloniki, 54124 Thessaloniki, Greece

ARTICLE INFO

Article history:
Received 13 April 2017
In final form 25 May 2017
Available online 26 May 2017

ABSTRACT

The photopolymer formation in the fullerene layers of the C_{60} complex with platinum dibenzyldithiocarbamate is reported for the first time. The photo-oligomer peaks appear in the Raman spectra near the $A_g(2)$ mode of the C_{60} molecule upon sample illumination with various laser wavelengths. The photo-oligomers are unstable upon heating and revert back to the C_{60} monomeric state. The activation energy of the thermal decomposition, obtained from the Arrhenius dependence of the decay time constant on temperature, is (1.12 ± 0.11) eV and the photo-oligomers decompose at ~130 °C, being more fragile than the crystalline polymers of C_{60}.

© 2017 Elsevier B.V. All rights reserved.

1. Introduction

The polymerization of pristine C_{60} under illumination by visible light occurs in thin films or surfaces of bulk samples, owing to the small penetration depth of the light, resulting in a rather disordered material consisting of various photo-oligomers [1–3]. Covalent bonds among adjacent fullerene molecules arise due to a [2+2] cyclo-addition mechanism [4]. On the other hand, the treatment of C_{60} fullerene under various conditions of high pressure and high temperature (HPHT) results in the formation of bulk ordered crystalline polymers. X-ray diffraction (XRD) studies of carefully prepared HPHT fullerene polymers have identified their crystal structures as one-dimensional orthorhombic (1D-O), two-dimensional tetragonal (2D-T) and two-dimensional rhombohedral (2D-R) [5,6]. The IR absorption and Raman scattering studies of fullerene polymers show the splitting and softening of the intramolecular modes of C_{60} due to the formation of intermolecular covalent bonds and the concomitant symmetry and molecular stiffness reduction [7,8]. Spectroscopic examination of the C_{60} polymers is mainly based on the behavior of the $A_g(2)$ pentagon-pinch (PP) mode of the C_{60} cage, corresponding to the in-phase stretching vibration that involves tangential displacements of carbon atoms with a contraction of the pentagonal rings and an expansion of the hexagonal rings. In the C_{60} polymers, the PP-mode downshifts due to the decrease of the mean intramolecular bond strength. The softening depends on the number of the sp^3-like coordinated carbon atoms per C_{60} molecular cage, associated with the intermolecular covalent bond formation. The $A_g(2)$ mode of the *fcc* C_{60} monomer appearing at 1468 cm^{-1} downshifts to 1458 cm^{-1} in the 1D-O polymer (4 sp^3-like coordinated carbon atoms). In the 2D-T polymer (8 sp^3-like coordinated carbon atoms), the peak further downshifts to 1446 cm^{-1}, while in the case of the 2D-R phase (12 sp^3-like coordinated carbon atoms) the $A_g(2)$ mode exhibits the largest softening and is observed at 1408 cm^{-1} [7–10].

Fullerene polymers are stable at ambient conditions but decompose at elevated temperatures reverting back to the monomer [6,11]. The stability of bulk C_{60} polymers at elevated temperature has been studied by differential scanning calorimetry (DSC) [12,13]. DSC measurements show a strong endothermic peak between 252 °C and 292 °C during the heating scan [12]. The transition temperature depends on the polymeric phase and somewhat on the scanning rate, indicating that the polymer decomposition process is controlled by kinetics. The decomposition kinetics of bulk crystalline polymers was studied by XRD, IR absorption and Raman scattering measurements [11,14–16]. The small amount of the C_{60} photopolymers on the surface of the samples makes DSC measurements and structural analysis methods inapplicable for their study. Thus, Raman spectroscopy becomes a unique tool in the study of the photopolymer formation and the decomposition kinetics of the photopolymers at elevated temperature.

In this work, we report the first observation of the photopolymer formation in the fullerene layers of the molecular donor-acceptor complex of C_{60} with platinum dibenzyldithiocarbamate

* Corresponding author.
E-mail address: jarvan@physics.auth.gr (J. Arvanitidis).

http://dx.doi.org/10.1016/j.cplett.2017.05.065
0009-2614/© 2017 Elsevier B.V. All rights reserved.

({Pt(dbdtc)$_2$}·C_{60}, chemical formula $C_{30}H_{28}PtN_2S_4{\cdot}C_{60}$). The complex possesses layered structure in which the close-packed fullerene layers with nearly hexagonal arrangement of C_{60} molecules alternate with layers of platinum dibenzyldithiocarbamate molecular donors. The photopolymerization, manifested by the appearance of a number of new peaks in the frequency region of the PP-mode, is very fast under laser illumination at λ_{exc} = 515 nm even for power as low as 1 μW, while it becomes much slower under 160 μW at λ_{exc} = 785 nm. The frequencies of the newly appearing PP-mode components are very close to those of the various crystalline polymers with different number of sp^3-like coordinated carbon atoms per C_{60} cage [7–10]. The intensity of these bands gradually increases with illumination time, while the photopolymer content can be inferred by the ratio of the sum of the integrated intensities of the new PP-mode components to the total spectral intensity in the frequency region of the PP-mode. The output of the photopolymer grows exponentially with the laser irradiation time, with the exponential growth time constant decreasing at elevated laser power and the process becoming faster. In addition, the abrupt change of the sample volume due to the higher density of the photopolymer causes high local stress and leads to the appearance of visible cracks on the surface of the sample. The photopolymer obtained in this way is stable at ambient conditions but under heating it reverts back to the monomer, similarly to the case of the crystalline fullerene polymers. The kinetics of the photopolymer decomposition was studied at elevated temperature by Raman spectroscopy with λ_{exc} = 785 nm and 20 μW on the polymeric samples previously formed under laser illumination at λ_{exc} = 785 nm with 1.2 mW. The activation energy of the photopolymer decomposition, obtained from the Arrhenius dependence of the exponential decay time constant on the temperature, is (1.12 ± 0.11) eV while the photo-oligomers revert back to the monomer within 15 min at ~130 °C. These values are considerably smaller than those of the crystalline polymers of C_{60}, indicating that the photo-oligomers in the fullerene layers of the {Pt(dbdtc)$_2$}·C_{60} complex are less stable than the crystalline polymers of C_{60} [12–16].

2. Experimental

The samples of the {Pt(dbdtc)$_2$}·C_{60} complex were obtained by the evaporation of a solution containing fullerene C_{60} and platinum dibenzyldithiocarbamate following a procedure described elsewhere [17]. The {Pt(dbdtc)$_2$}·C_{60} complex adopts a monoclinic structure (space group $P2_1/c$). The parameters of the unit cell are a = 15.957(5), b = 17.241(5), c = 10.018(5) Å, β = 92.356(5)° and V = 2753.7(5) Å^3. The fullerene molecules at ambient conditions are in monomeric state forming a layered structure. Within the fullerene layers, each C_{60} molecule is surrounded by six C_{60} neighbors with the shortest distances between the centers of the molecules being 9.97 (four neighbors) and 10.02 Å (two neighbors). The platinum dibenzyldithiocarbamate molecules are arranged between the fullerene layers by benzyl substituent's, while no covalent or coordination bonds were found between Pt(dbdtc)$_2$ and C_{60} [18].

The samples of the {Pt(dbdtc)$_2$}·C_{60} complex were well-facetted crystals with mirror-like surfaces and in-plane dimensions between 50 and 300 μm. The Raman spectra were recorded in the backscattering geometry using LabRam HR and LabRam ARAMIS (HORIBA) micro-Raman spectrometers, as well as an Acton SpectraPro-2500i spectrograph, all equipped with Peltier cooled CCD detectors. Lasers at 515, 532, 633 and 785 nm and Olympus 50× and 100× objectives were used for the photopolymer formation and Raman probing. The Raman spectra of the fullerene molecular complexes are identical to those of the C_{60} molecule due to the considerably higher Raman cross-section of fullerene acceptor with respect to the molecular donor [19]. In addition, the absorption spectra of the fullerene complexes are close to those of the pristine C_{60}, characterized by strong absorption in the UV and visible regions and a weak absorption tail in the far red and near infrared regions [17]. The Raman measurements at elevated temperatures were performed using a high temperature cell with a quartz window. The cell was equipped with a temperature controller unit that maintains temperatures up to 380 °C with an accuracy of ±2 °C. The heating and cooling rates in the temperature range of interest were ~15 °C/min and ~10 °C/min, respectively. The photopolymer samples were prepared at ambient temperature inside the temperature cell by laser treatment of a 10 × 10 μm^2 area on the surface of the sample, taking advantage of the DuoScan™ (HORIBA) system, using laser irradiation at λ_{exc} = 785 nm and 1.2 mW focused in a spot of ~2 μm through a 50× long working distance objective for 2–3 h. Raman probing (λ_{exc} = 785 nm, 20 μW) of the polymer decomposition time kinetics at high temperature was performed by averaging signal from the central part (5 × 5 μm^2) of the laser treated area to avoid any erroneous signal from minute displacements of the sample at high temperature. The Raman measurements were performed in air; however, Raman measurements performed in the evacuated volume of a continuous flow liquid helium cryostat as well as in ethanol/methanol mixture inside a high pressure diamond anvil cell (not presented here) have shown that the results do not depend on the sample environment.

3. Results and discussion

Fig. 1 depicts the phototransformation of the {Pt(dbdtc)$_2$}·C_{60} complex at ambient conditions and 1 μW laser power at λ_{exc} = 515 nm using the 100× objective. The left inset in Fig. 1 shows the molecular arrangement in the lattice of the {Pt(dbdtc)$_2$}·C_{60} complex. The Raman spectra, collected for 120 s each, after 120, 360, 600 and 940 s of continuous laser irradiation, are illustrated in the right inset of Fig. 1. In the frequency region of the PP-mode, new rather sharp bands appear with frequencies very close to the corresponding PP-bands of the various crystalline polymers of C_{60} having different numbers of sp^3-like coordinated carbon atoms per molecular cage. The phototransformation is also accompanied by the splitting of the H_g five-fold degenerate modes

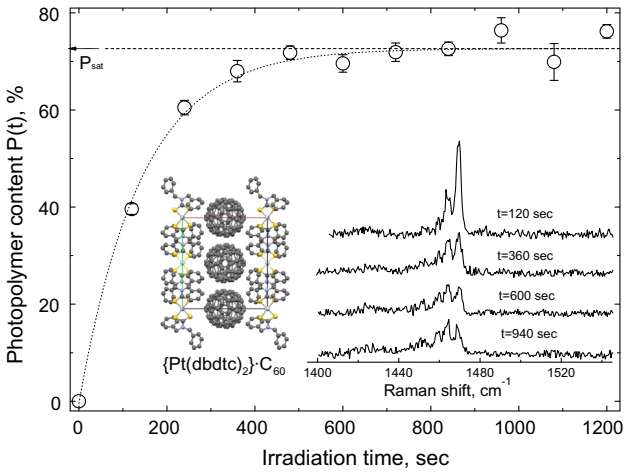

Fig.1. Photopolymer content in the {Pt(dbdtc$_2$)}·C_{60} complex, excited through a 100 × objective at λ_{exc} = 515 nm with a laser power of 1 μW, as a function of the irradiation time (circles), fitted by an exponential growth function (dotted line). Left inset: Molecular arrangement in the fullerene complex viewed along the a-axis of the unit cell. Right inset: Time evolution of the Raman spectra in the frequency region of the PP-mode.

of the C_{60} molecule (not shown in the figure). The intensity of the new bands increases with the laser irradiation time while the intensity of the initial PP-mode decreases. The ratio of the sum of the integrated intensities of the new PP-mode components to the total spectral intensity in this frequency region (fractional intensity) provides a measure of the photopolymer content. The dependence of the photopolymer content on the laser irradiation time is also shown in Fig. 1 (circles) along with the fitting of experimental data by an exponential growth function (dotted line):

$$P(t) = P_{sat} \times \{1 - \exp(-t/\tau)\} \quad (1)$$

where P(t) is the time-dependent content of the photopolymer, P_{sat} is the content of the photopolymer attained after saturation of the phototransformation process, and τ is the exponential growth time constant. The phototransformation constants are $P_{sat} = 73\%$ and $\tau = 141$ s for the aforementioned experimental conditions. Note, that the polymer content after saturation, P_{sat}, is always less than 100%. This may be related to the small uncontrolled shift of samples during the Raman measurements under conditions of sharp beam focusing. Nevertheless, the competition between the polymer formation and polymer decomposition processes, both caused by the laser irradiation, cannot be excluded. It is well known that the temperature of the sample in the laser spot area exceeds the bath temperature due to the laser overheating effect [20]. The elevated temperature activates the polymer decomposition that occurs simultaneously, counteracting the light induced polymer formation and eventually leading to an equilibrium where the polymer is only partially phototransformed. In fact, the temperature within the laser spot on the sample, the saturation level P_{sat} and the time constant τ depend on the laser power density that implies the necessity of careful focusing of the laser beam on the sample in order to obtain reproducible data. Similar results were also obtained with excitations at 532 and 633 nm (not shown).

The phototransformation process is less pronounced for excitation in the far red - near infrared spectral region because the penetration depth is much larger (smaller absorption coefficient) [20]. Fig. 2 depicts the evolution of the Raman spectra of the {Pt(dbdtc$_2$)}·C_{60} complex under prolonged laser irradiation at $\lambda_{exc} = 785$ nm with laser power at 16 and 160 μW using the 100× objective. The right inset in Fig. 2 depicts the Raman spectra of the {Pt(dbdtc$_2$)}·C_{60} complex measured at a laser power of 16 μW. The five spectra recorded consecutively under irradiation time up to 3000 s with 600 s measurement time for each spectrum do not exhibit any observable changes. Note, that the laser power density in this case is ~1400 W/cm^2, exceeding ~7 times the power density of ~200 W/cm^2 for the case of the laser excitation with 515 nm and 1 μW. Nevertheless, the photopolymerization in the case of the 785 nm excitation is hindered due to the smaller absorbance. The left inset in Fig. 2 depicts the Raman spectra of the {Pt(dbdtc$_2$)}·C_{60} complex measured while irradiated at a laser power of 160 μW. The spectra were acquired consecutively up to 3600 s with a measurement time of 300 s each. The increase of the laser power activates the phototransformation process and the new bands gradually appear near the PP-mode of the pristine (monomeric) material. The photopolymer content as a function of the laser irradiation time is also shown in Fig. 2 (circles) along with the fitting of experimental data by an exponential growth function (dotted line). The experimental dependence contains two components that can be fitted by two exponential growth functions. In the first region up to ~2400 s, the dependence is well fitted by Eq. (1) with $P_{sat1} = 45\%$ and $\tau = 320$ s. The next region from 2400 to 3600 s is fitted by the function:

$$P(t) = P_{sat1} + P_{sat2} \times \{1 - \exp\{-(t - t_{cr}/\tau)\}\} \quad (2)$$

where $P_{sat2} = 70\%$, $t_{cr} = 2400$ s and $\tau = 392$ s. As it can be inferred from the figure, the photopolymer content is strongly affected by a crack on the sample surface that appears after ~2400 s of laser irradiation with a power of 160 μW (see the micrographs in Fig. 2). Evidently, the balance between the photoinduced polymerization process and the thermal decomposition is disturbed in favor of the former by the crack formation and the changes in the laser focusing.

Fig. 3 shows the frequencies of the Raman peaks originating from the PP-mode of the C_{60} molecule in the various HPHT polymers of C_{60} (circles) *vs* the number of the sp^3-like coordinated carbon atoms per C_{60} molecular cage [7–10,21]. The frequencies of the split PP-mode components in the photopolymerized {Pt(dbdtc$_2$)}·C_{60} complex (open stars) are also shown in the figure. The structural arrangements of the intermolecular covalent bonds in the different HPHT crystalline polymers, as deduced by detailed XRD

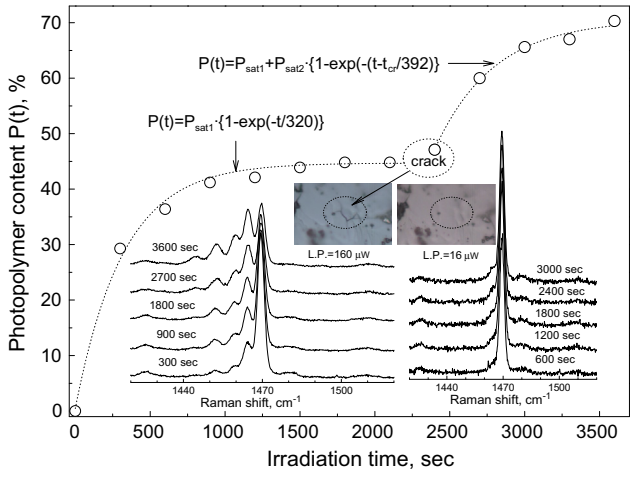

Fig.2. Photopolymer content in the {Pt(dbdtc$_2$)}·C_{60} complex, excited through a 100 × objective at $\lambda_{exc} = 785$ nm with a laser power of 160 μW, as a function of the laser irradiation time (circles), fitted by an exponential growth function (dotted line). Insets: Time evolution of the Raman spectra of the {Pt(dbdtc$_2$)}·C_{60} complex in the frequency region of the PP-mode excited through a 100 × objective at $\lambda_{exc} = 785$ nm with laser power 16 μW (right) and 160 μW (left), as well as micrographs illustrating a crack formed on the sample surface at the higher laser power.

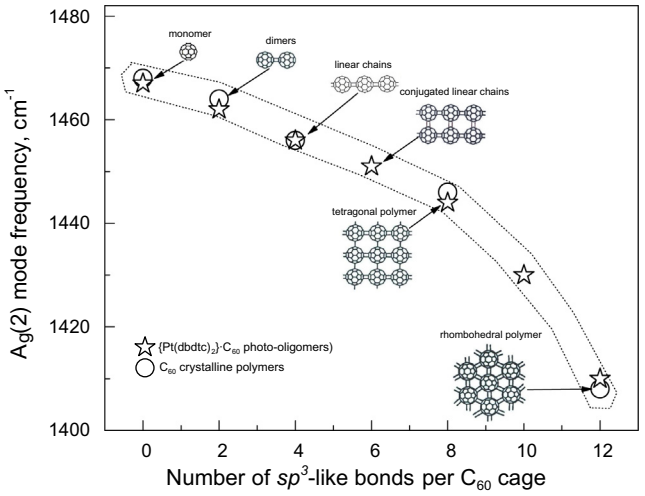

Fig.3. The frequencies of the PP-mode in the HPHT crystalline polymers of C_{60} (circles) and the corresponding PP-components in the photo-transformed {Pt(dbdtc$_2$)}·C_{60} complex (stars). The number of the sp^3-like coordinated carbon atoms per C_{60} molecular cage. The arrangement of the intermolecular covalent bonds in the various HPHT crystalline polymers is also shown.

measurements, are illustrated in the figure insets [5,6,22]. The empirical dependence plotted in Fig. 3 shows a gradual decrease of the PP-mode frequency of the HPHT polymers of C_{60} with the increase in the number of the sp^3-like coordinated carbon atoms per C_{60} molecule. The frequencies of the new PP-mode components in the photopolymerized {Pt(dbdtc)$_2$}·C_{60} complex agree well with those of the crystalline polymers, suggesting their origin as photo-oligomers related to dimers, fragments of linear chains, conjugated linear chains, planar tetragonal and rhombohedral polymeric networks. Assuming that the Raman scattering cross-section does not change significantly upon the formation of the sp^3-like intermolecular bonds, the intensities of the various components of the studied fullerene complex after saturation of photopolymerization indicate that the resulting material contains C_{60} dimers, fragments of linear chains, conjugated linear chains and planar tetragonal polymers in approximately equal concentrations. This is possibly related to the tetragonal arrangement of the nearest neighboring C_{60} molecules within the fullerene layers of the complex. Note, that the long time exposure at λ_{exc} = 515 nm and 36 μW (spectra not shown) leads to stronger polymerization and redistribution of the PP-mode component intensities. In this case, the intensities of the peaks at 1444 and 1432 cm^{-1} considerably increase and a weak shoulder appears near 1410 cm^{-1}. The peaks at 1444 and 1410 cm^{-1} correspond to the tetragonal and rhombohedral polymer, while the one at ~1432 cm^{-1} could be attributed to the PP-mode of an exotic photo-oligomer with 10 sp^3-like coordinated carbon atoms per fullerene molecular cage. However, the assignment of this peak to a split component of the $H_g(7)$ mode cannot be excluded [23,24]. Furthermore, the Raman band at ~1451 cm^{-1} in the phototransformed {Pt(dbdtc)$_2$}·C_{60} complex does not exist in the crystalline polymers of C_{60} and is related to conjugated linear chains that were observed under pressure- and photo-induced transformations in the linear orthorhombic polymer of C_{60} [21,22].

The stability of the photo-oligomers in the {Pt(dbdtc)$_2$}·C_{60} complex at elevated temperatures and the kinetics of their decomposition under heating were studied in the temperature range 95–120 °C. The Raman spectra, measured at λ_{exc} = 785 nm with a laser power of 20 μW and using a 50× objective during the thermal treatment of a new, freshly photopolymerized sample for each temperature, show a gradual decomposition of the photopolymer content with treatment time. Note, that the estimation of the sample overheating made on the basis of Ref. 20 for the pristine C_{60} at 20 μW, λ_{exc} = 515 nm and 50× objective shows that the temperature in the laser spot exceeds the bath temperature by ~12 °C. However, the overheating in our case is considerably smaller because the absorbance at λ_{exc} = 785 nm is about thirty times smaller than that at λ_{exc} = 515 nm. The inset of Fig. 4 illustrates the Raman spectra of the photo-polymerized {Pt(dbdtc)$_2$}·C_{60} complex in the region of the PP-mode recorded consecutively with a measurement time of 180 s for each spectrum during the thermal treatment at 95 °C for ~4 h. The lower Raman spectrum depicts the photo-oligomers in the {Pt(dbdtc)$_2$}·C_{60} complex at room temperature formed after intense laser irradiation with 1.2 mW (λ_{exc} = 785 nm and 50× objective) for more than 2 h. This spectrum exhibits the typical features of the photopolymer and is characterized by a significantly reduced monomeric PP-component, while the corresponding dimeric one is dominant. The rest of the spectra correspond to the photo-oligomers treated at 95 °C for 180, 3300, 7380 and 13,290 s. The intensity of the photo-oligomers PP-components decreases with the treatment time whereas that of the monomers increases. The last spectrum, recorded after 13,290 s of thermal treatment, corresponds to almost monomeric C_{60}. Open circles in Fig. 4 depict the fractional intensity of the PP-mode components of the photo-oligomers in the {Pt(dbdtc)$_2$}·C_{60} complex as a function of the thermal treatment time, whereas

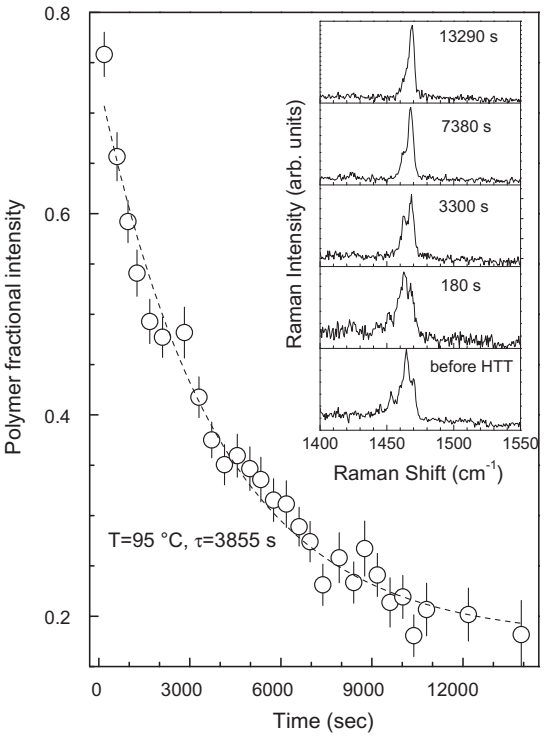

Fig.4. The fractional intensity of the photo-oligomers in the photo-transformed {Pt(dbdtc)$_2$}·C_{60} complex as a function of the thermal treatment time at 95 °C (circles) and the fit of the experimental data by an exponential decay function (dotted line). Inset: Time evolution of the Raman spectra in the frequency region of the PP-mode during the thermal treatment.

the dotted line is the fit of the experimental data by an exponential decay function:

$$P(t) = P_{res} + P_0 \times \exp(-t/\tau) \quad (3)$$

where the P(t) is the time-dependent content of the photo-oligomers under thermal treatment, P_0 is the initial polymer content that was attained after saturation of the photopolymerization (P_{sat}), P_{res} is the residual content of the photopolymer after saturation of the decomposition process, which decreases with increasing temperature, and τ is the exponential decay time constant. The decomposition time constant at 95 °C is τ = 3855 s while the residual polymer content is P_{res} = 17%. It is interesting to note that although photopolymerization always leads to crack formation on the sample surface, thermal treatment partially restores the surface due to the volume expansion upon recovering of the initial monomeric C_{60} state.

Fig. 5 illustrates the kinetics of the photo-oligomer decomposition at various treatment temperatures. Circles represent the experimental data while dotted lines are fits to the data by the exponential decay function given in Eq. (3). The photo-oligomers decompose faster at higher treatment temperatures. Namely, at 100 °C the exponential decay time constant decreases to 3561 s while P_{res} also decreases to ~13%. At 105 °C the decay time constant decreases to 1680 s while further increase of the temperature treatment to 120 °C makes the polymer decomposition very rapid: the decay time constant decreases to 508 s while P_{res} drops to ~1%. The decrease of the decay time constant with the increase of the treatment temperature indicates the activation-type behavior of the photo-oligomers decomposition. This behavior is typical for chemical reactions and was observed for the thermal decomposition of all fullerene polymers [14–16]. The activation energy of the photo-oligomer decomposition can be estimated taking into

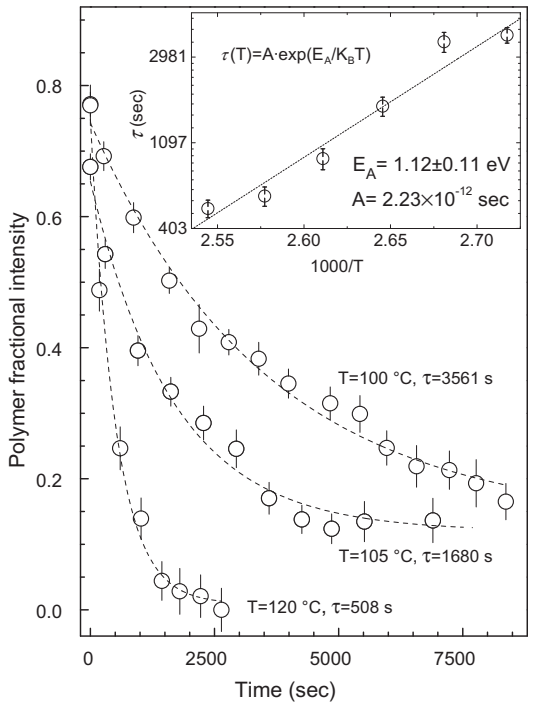

Fig. 5. Time dependence of the fractional intensity of the photo-oligomers in the photo-transformed $\{Pt(dbdtc)_2\}\cdot C_{60}$ complex at treatment temperatures 100, 105 and 120 °C (circles) and the fits of the experimental data by exponential decay functions (dotted lines). Inset: Arrhenius dependence of the exponential decay time constant on the treatment temperature.

account the Raman data regarding the dependence of the exponential decay time constant on the treatment temperature. This dependence can be described by the Arrhenius equation:

$$\tau(T) = A \times \exp(E_A/k_B T) \quad (4)$$

where E_A is the activation energy (energy barrier between the photopolymer and monomer states), k_B is the Boltzmann constant, T is the treatment temperature and τ the exponential decay time constant. The constant A, related to the characteristic phonon frequency, is measured in time units [14]. The corresponding Arrhenius plot is also included in Fig. 5 as inset. The experimental data exhibit a linear dependence in logarithmic scale, yielding an activation energy of $E_A = 1.12 \pm 0.11$ eV/molecule. This value is smaller than the activation energies of the thermal decomposition of dimers, linear and planar polymers, ranging between 1.75 and 1.9 eV/molecule [14,16]. On the other hand, it is close to the activation energy $E_A = 1.25$ eV/molecule of the thermal decomposition of photopolymerized C_{60} also obtained by Raman scattering measurements [11]. Using the values of the activation energy E_A and the constant A obtained from the Arrhenius equation we calculated the temperature for the photopolymer content to drop to 1% (complete decomposition) within 15 min of thermal treatment to be ~130 °C. Note that the time estimated for the photo-oligomer decomposition to 1% at room temperature is about 10^5 times larger. On the other hand, the temperatures for the complete decomposition of crystalline dimers, linear and planar polymers range between 175 °C and 280 °C [12,14,25]. Thus, the photo-oligomers originating from the $\{Pt(dbdtc)_2\}\cdot C_{60}$ complex are less stable than the crystalline HPHT polymers of C_{60} and the photopolymerized one. The weaker covalent bonding between the adjacent C_{60} molecules in the fullerene complex could be related to the planar arrangement of the fullerene molecules in the crystal structure of the complex, in which the platinum dibenzyldithiocarbamate molecular layers separate the fullerene ones.

Summarizing, we have studied the photopolymerization in the C_{60} layers of a fullerene donor-acceptor complex at ambient conditions. The photopolymerization rate in the $\{Pt(dbdtc)_2\}\cdot C_{60}$ complex and the polymer content attained after saturation of the phototransformation depend on the excitation wavelength and the laser power density. The photo-oligomers are, most likely, dimers, fragments of linear chains, conjugated linear chains, as well as planar polymeric networks. The Raman study of the decomposition kinetics of the photo-oligomers at elevated temperature yields an activation energy of (1.12 ± 0.11) eV/molecule. This value is considerably smaller than those for the thermal decomposition of dimers, linear and planar polymers that range between 1.71 and 1.9 eV/molecule, estimated by XRD and Raman measurements at elevated temperatures. The estimated temperature for the complete decomposition of the photo-oligomers is ~130 °C that is considerably smaller than those for crystalline HPHT C_{60} dimers (~180 °C) and linear and planar polymers (~280 °C). Thus, the covalent intermolecular bonds between the C_{60} molecules in the fullerene complex are weaker than those in the HPHT polymers of C_{60}. The formation of the HPHT crystalline polymers is a more energy demanding process due to bulk structural transformations and deformation of the fullerene molecular cages whereas the photopolymerization in the $\{Pt(dbdtc)_2\}\cdot C_{60}$ complex requires less energy due to the separation of fullerene layers by $Pt(dbdtc)_2$, as well as the small size and the disordered structure of the resulting fullerene photo-oligomers.

Acknowledgments

The authors are grateful to Dr. D. Konarev for providing the fullerene complexes. Authors are also thankful to the Center of Interdisciplinary Research and Innovation of the Aristotle University of Thessaloniki (ΚΕΔΕΚ) for the access to the Raman instrumentation. KPM acknowledges the main financial support by the Federal Agency for Scientific Organizations, the partial support by the Russian Foundation for Fundamental Research, grant No. 15-02-01495, and the RAS Presidium Program "Physics of compressed matter", as well as the hospitality of the Aristotle University of Thessaloniki.

References

[1] A.M. Rao, P. Zhou, K.-A. Wang, G.T. Hager, J.M. Holden, Y. Wang, W.T. Lee, X.X. Bi, P.C. Ecklund, D.S. Cornett, Science 259 (1993) 955.
[2] T. Pusztai, G. Oszlanyi, G. Faigel, K. Kamaras, L. Granasy, S. Pekker, Solid State Communications 111 (1999) 595.
[3] V.A. Karachevtsev, P.V. Mateichenko, N.Y. Nedbailo, A.V. Peschanskii, A.M. Plokhotnichenko, O.M. Vovk, E.N. Zubarev, A.M. Rao, Carbon 42 (2004) 2091.
[4] P. Zhou, Z.H. Dong, A.M. Rao, P.C. Ecklund, Chem. Phys. Lett. 211 (1993) 337.
[5] Y. Iwasa, T. Arima, R.M. Fleming, T. Siegrist, O. Zhou, R.C. Haddon, L.J. Rothberg, K.B. Lyons, H.L. Karter Jr., A.F. Hebard, R. Tycko, G. Dabbagh, J.J. Kraejewski, G.A. Thomas, T. Yagi, Science 264 (1994) 1570.
[6] M. Nunez-Regueiro, L. Marques, J.-L. Hodeau, O. Bethoux, M. Perroux, Phys. Rev. Lett. 74 (1995) 278.
[7] J. Winter, H. Kuzmany, A. Soldatov, P.-A. Persson, J. Jacobsson, B. Sundqvist, Phys. Rev. B 54 (1996) 17486.
[8] A.M. Rao, P.C. Ecklund, J.-L. Hodeau, L. Marques, M. Nunez-Regueiro, Phys. Rev. B 55 (1997) 4766.
[9] T. Wägberg, P. Jacobsson, B. Sundqvist, Phys. Rev. B 60 (1999) 4535.
[10] V.A. Davydov, L.S. Kashevarova, A.V. Rakhmanina, V.M. Senyavin, R. Ceolin, H. Szwarc, H. Allouchi, V. Agafonov, Phys. Rev. B 61 (2000) 11936.
[11] Y. Wang, J.M. Holden, X.-X. Bi, P.C. Eklund, ChemPhys. Lett. 217 (1994) 413.
[12] Y. Iwasa, K. Tanoue, T. Mitani, T. Yagi, Phys. Rev. B 58 (1998) 16374.
[13] M.V. Korobov, A.G. Bogachev, A.A. Popov, V.M. Senyavin, E.B. Stukalin, A.V. Dzyabchenko, V.A. Davydov, L.S. Kashevarova, A.V. Rakhmanina, V. Agafonov, Carbon 43 (2005) 954.
[14] P. Nagel, V. Pasler, S. Lebedkin, A. Soldatov, C. Meingast, B. Sundqvist, P.-A. Persson, T. Tanaka, K. Komatsu, S. Buga, A. Inaba, Phys. Rev. B 60 (1999) 16920.
[15] T. Wägberg, P.-A. Persson, B. Sundqvist, P. Jacobsson, Appl. Phys A 64 (1997) 223.
[16] K.P. Meletov, J. Arvanitidis, D. Christofilos, G.A. Kourouklis, Y. Iwasa, S. Yamanaka, Carbon 48 (2005) 2974.

[17] D. V. Konarev, S. S. Khasanov, D. V. Lopatin, V. V. Rodaev, and R. N. Lyubovskaya, Russ. Chem. Bull., Int. Ed. 56 (2007) 2145.
[18] K.P. Meletov, D.V. Konarev, Chem. Phys. Lett. 553 (2012) 21.
[19] K.P. Meletov, Phys. Solid State 56 (2014) 1689.
[20] K.P. Meletov, E. Liarokapis, J. Arvanitidis, K. Papagelis, D. Palles, G.A. Kourouklis, S. Ves, Chem. Phys. Lett. 290 (1998) 125.
[21] K.P. Meletov, V.A. Davydov, A.V. Rakhmanina, V. Agafonov, G.A. Kourouklis, Chem. Phys. Lett 416 (2005) 220.
[22] R. Le Parc, C. Levelut, J. Haines, V.A. Davydov, A.V. Rakhmanina, R.J. Papoular, E. E. Belova, L.A. Chernozatonskii, H. Allouchi, V. Agafonov, Chem. Phys. Lett. 438 (2007) 63.
[23] R. Moret, P. Launois, T. Wägberg, B. Sundqvist, Eur. Phys. J. B 15 (2000) 253.
[24] T. Wägberg, B. Sundqvist, Phys. Rev. B 95 (2002) 11542.
[25] G.-W. Wang, K. Komatsu, Y. Murata, M. Shiro, Nature 387 (1997) 583.